Effects of Aluminium Oxide Content on the Regenerated Magnesia-Calcium Bricks for Cement Rotary Kiln

Gui-bo Qiu , Yi-dang Hao , Jia Hou , Hui-gang Wang , Xuan-hao Zhang , Ben Peng * , Mei Zhang *

Posted Date: 14 September 2023

doi: 10.20944/preprints202309.0890.v1

Keywords: regenerated magnesia-calcium bricks; aluminium oxide; microstructure; flexural strength; corrosion resistance; coating adherence

Article

Effects of Aluminium Oxide Content on the Regenerated Mag-Nesia-Calcium Bricks for Cement Rotary Kiln

Gui–bo Qiu [1,2,3,4], Yi–dang Hao [1,2,3,5], Jia Hou [1,2,3,4], Hui–gang Wang [1,3,4,5], Xuan–hao Zhang [1,2,3,4], Ben Peng [1,5,*] and Mei Zhang [3,4,6,*]

1 Central Research Institute of Building and Construction Co., Ltd. MCC Group, Beijing, 100088, China; qiuguibo@cribc.com (Q.G.-B.); haoyidang@cribc.com (H.Y.-D.); houjia@cribc.com (H.J.); wanghuigang0822@126.com (W.H.-G.); 892541615@qq.com (Z.X.-H.)
2 Zhanjiang Environmental Protection Operation Management Co., Ltd, MCC Group, Zhanjiang, 524000, China
3 Guangdong Iron and Steel Smelting Resource Comprehensive Utilization Engineering Technology Research Center, Zhanjiang, 524000, China
4 Zhanjiang Key Laboratory of Environmental Protection for Metallurgical Industry, Zhanjiang, 524000, China
5 Energy conservation and environment protection CO., LTD, MCC Group, Beijing, 100088, China
6 School of Metallurgical and Ecological Engineering, University of Science and Technology Beijing, Beijing, 100083, China
* Correspondence: pengben@cribc.com (P.B.); zhangmei@ustb.edu.cn (Z.M.)

Abstract: The regenerated magnesia-calcium brick samples that had added 0, 1.5, 3.0 wt.% aluminium oxide (Al_2O_3) were prepared by using spent magnesia-calcium bricks, fused magnesia and Al_2O_3 powder additive as the main raw materials. The phases, microstructures, room temperature and hot flexural strength, resistance to cement clinker corrosion and strength of coating adherence were investigated respectively. It indicated that the addition of Al_2O_3 increased mainly resulting in the content of tetracalcium aluminoferrite (C_4AF) and tricalcium aluminate (C_3A) increased in the regenerate samples. The bulk density, the room temperature flexural strength and the strength of coating adherence all increased, while the hot flexural strength and corrosion resistance both deteriorated along with the increase of Al_2O_3 addition. It was because that on the one hand the low melting point phases of C_4AF and C_3A improved the sinterability of the regenerated samples during the burning stage, on the other hand they melted or existed in liquid phase during the experimental temperature (1573 K and 1823 K) which degraded hot flexural strength and corrosion resistance, and enhanced the strength of coating adherence as the wettability of the liquid phase. The content of Al_2O_3 in the regenerated magnesia-calcium brick should not be higher than 1.1 wt.%, considering its room and high-temperature performances for cement rotary kiln.

Keywords: regenerated magnesia-calcium bricks; aluminium oxide; microstructure; flexural strength; corrosion resistance; coating adherence

1. Introduction

Currently, magnesite-chrome bricks have been widely used in cement rotary kiln in China [1]. It has led to serious environmental problems, because the Cr(Ⅲ) is easily oxidized into the toxic Cr(Ⅵ) in magnesite-chrome bricks under natural condition [2], especially spent magnesite-chrome bricks have not been reasonably handle. Therefore, it's urgently to develop free chrome refractory bricks to substitute for magnesite-chrome bricks in cement rotary kiln [3–5].

Magnesia-calcium bricks have been widely used as lining materials in ferrous metallurgy to produce the clean steel such as refining furnace [6], because of their excellent performances [7]. They are also regarded as the substitution of magnesite-chrome bricks for cement rotary kiln [8], because they own the similar operational performances, such as high–temperature resistance, corrosion

 doi:10.20944/preprints202309.0890.v1

resistance and good coating adherence, etc. [9,10]. However, the application of magnesia-calcium bricks on cement rotary kiln has been restricted, since they have bad hydration resistance which can result in seriously structural damage [11]. Related researches showed that aluminium oxide (Al_2O_3) could enhance the hydration resistance of magnesia-calcium bricks [12–14].

There are more and more spent magnesia-calcium bricks not being reused effectively [15], because of high impurity content such as Al_2O_3 that can reduce the usability of regenerated product, and further leads to a new environmental problem. Besides, there was very rare study on the utilization of spent magnesia-calcium bricks [15,16]. A kind of high hydration resistance regenerated magnesia-calcium brick was prepared basing on the spent magnesia-calcium bricks in previous work [14], without removing the impurities of Al_2O_3 in spent magnesia-calcium bricks. It has not only realized the high reutilization rate of spent magnesia-calcium bricks, but also provided a possible pathway using regenerated magnesia-calcium bricks in the cement rotary kiln to substitute for magnesite-chrome bricks. Nevertheless, high-temperature performances such as high temperature strength and refractoriness need be degraded because of excessive impurity content, particularly the content of Al_2O_3 [17,18].

Therefore, in this work, the regenerated magnesia-calcium bricks with different content of additive Al_2O_3 were prepared respectively. The investigation and comparative of their phases, microstructures, room temperature and hot flexural strength, resistance to cement clinker corrosion and strength of coating adherence were carried out successively. This work can also provide a reference for the replacement of hazardous magnesite-chrome bricks in the cement rotary kiln by the regenerated magnesia-calcium bricks.

2. Materials and Methods

2.1. Main Raw Materials of the Regenerated Magnesia-Calcium Bricks

The main raw materials of the regenerated magnesia-calcium bricks were spent magnesia-calcium bricks, fused magnesia and Al_2O_3 powder additive. The spent magnesia-calcium bricks were from a refining furnace in ferrous industry, the fused magnesia was from a refractory materials plant, and Al_2O_3 powder additive was a kind of analytical reagent. Their chemical compositions were measured by an 1800 X-ray fluorescence spectrometer (XRF) and the results were shown in Table 1.

Table 1. Compositions of the main raw materials of the regenerated magnesia-calcium bricks (wt.%).

Constituents	MgO	CaO	SiO_2	Fe_2O_3	Al_2O_3
Spent magnesia-calcium bricks	58.18	33.92	2.81	2.68	1.51
Fused magnesia	94.16	1.63	2.64	1.00	0.27
Al_2O_3 powder	–	–	0.30	0.03	98.75

2.2. Preparation of the Regenerated Magnesia-Calcium Brick Samples

Figure 1 shows the synthetic process of the regenerated magnesia-calcium bricks. The mixture of the regenerated magnesia-calcium brick green body was prepared by using the main raw materials as show in Table 1, and liquid paraffin as the binder firstly. The green body was prepared by 100 MPa pressing the mixture to form a rectangular of 60 mm × 8 mm × 8 mm subsequently. The regenerated magnesia-calcium brick sample was obtained by firing the green body at 1873 K for 2 h under an air atmosphere finally. In this work, three kinds of regenerated magnesia-calcium brick green bodies containing 0 wt.%, 1.5 wt.%, 3.0 wt.% Al_2O_3 powder additive were prepared, their compositions were shown in Table 2, and their corresponding fired samples were marked as A0, A1.5, A3.0 respectively.

Preprints (www.preprints.org) | NOT PEER-REVIEWED | Posted: 14 September 2023 doi:10.20944/preprints202309.0890.v1

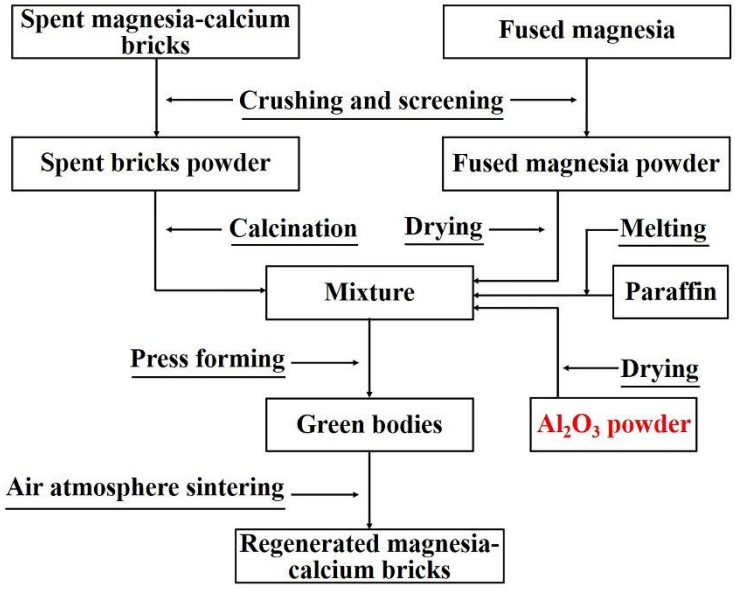

Figure 1. The synthetic process flow chart of regenerated magnesia-calcium bricks with Al_2O_3 powder addition.

Table 2. Compositions of the regenerated magnesia-calcium bricks' green bodies (wt.%).

Samples	MgO	CaO	SiO_2	Fe_2O_3	Al_2O_3	Al_2O_3 powder additive
A0	70	23.31	2.66	2.21	1.10	0
A1.5	70	23.31	2.66	2.21	1.10	1.5
A3.0	70	23.31	2.66	2.21	1.10	3.0

2.3. Characterization and Performance Test of the Regenerated Magnesia-Calcium Brick Samples

The phase compositions of the regenerated magnesia-calcium samples (regenerated samples) were identified by a MXP21VAHF X-ray powder diffractometry (XRD) analysis. The microstructures and elements distribution of the regenerated samples were investigated by an MLA 250-FEI Quanta scanning electron microscope (SEM) with an energy dispersive spectrometer (EDS). The room temperature flexural strength and strength of coating adherence of the regenerated samples were determined by a WDW–10E microcomputer controlled electronic universal testing machine. The hot flexural strength of the regenerated samples mechanical was determined by a CMT 5204 temperature-mechanical load coupling testing machine at 1573 K. The resistance to cement clinker corrosion and the coating adherence of the regenerated samples were investigated at 1823 K for 3 h as shown in Figure 2.

Preprints (www.preprints.org) | NOT PEER-REVIEWED | Posted: 14 September 2023 doi:10.20944/preprints202309.0890.v1

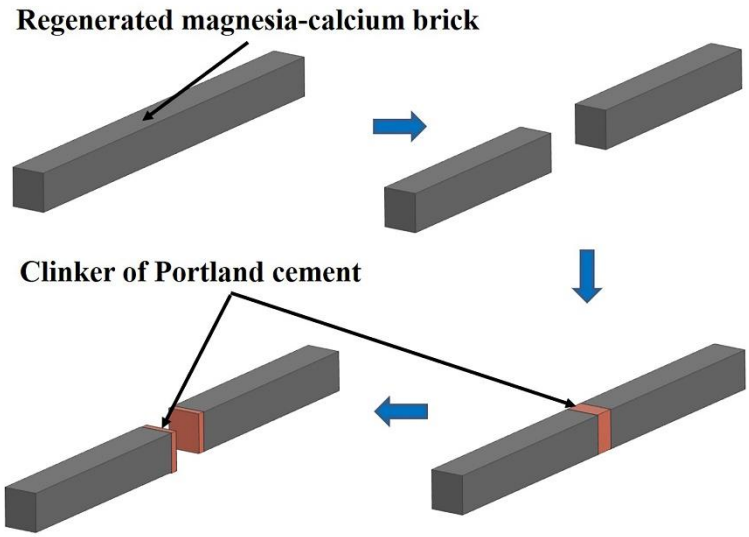

Figure 2. Schematic diagram of the resistance to cement clinker corrosion and the coating adherence experiment of the regenerated magnesia-calcium bricks.

3. Results

This section may be divided by subheadings. It should provide a concise and precise description of the experimental results, their interpretation, as well as the experimental conclusions that can be drawn.

3.1. Phase Compositions of the Regenerated Magnesia-Calcium Bricks

Figure 3(a) shows that the main phase compositions of the sample A0, A1.5 were identical the magnesia (MgO), free calcium oxide (f–CaO), tricalcium silicate (Ca_3SiO_5, C_3S) and tetracalcium aluminoferrite (Ca_2FeAlO_5, C_4AF), while the main phase compositions of the sample A3.0 were the MgO, f–CaO, C_3S, C_4AF and tricalcium aluminate ($Ca_3Al_2O_6$, C_3A). It shows that a new phase C_3A generated and other phases did not change according to the increase of Al_2O_3 addition in the regenerated samples.

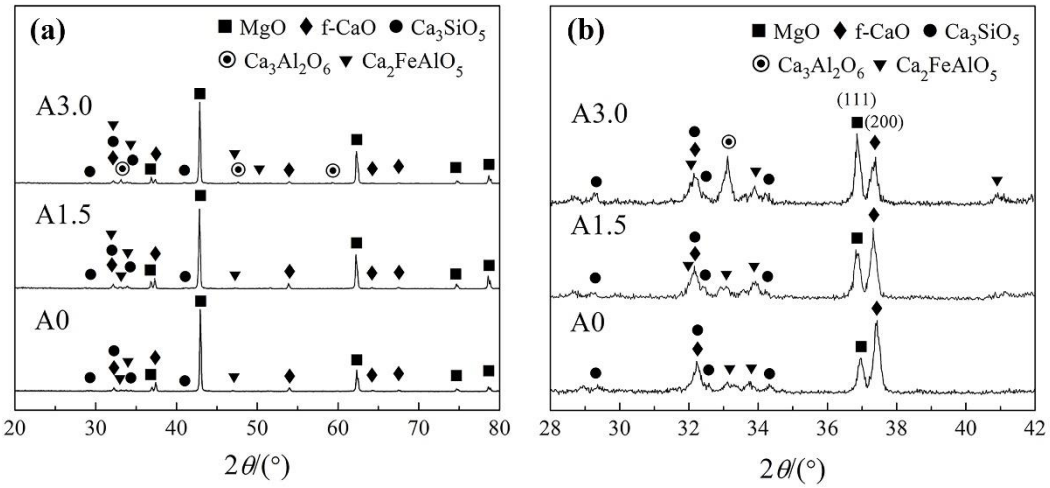

Figure 3. XRD patterns of the sample A0, A1.5 and A3.0: (**a**) the range of 20–80°; (**b**) the range of 28–42°.

Figure 3(b) shows that the intensity of character diffraction peaks of f–CaO [$I_{CaO(200)}$] and MgO [$I_{MgO(111)}$] were the two highest peaks in the range of 28–42° and varied significantly. The relative

Preprints (www.preprints.org) | NOT PEER-REVIEWED | Posted: 14 September 2023 doi:10.20944/preprints202309.0890.v1

intensities of $I_{CaO(200)}/I_{MgO(111)}$ decreased observably along with the increase of increase of Al_2O_3 addition in the regenerated magnesia-calcium bricks as shown in Figure 4. It also indicates that the content of f–CaO decreased along with the increase of Al_2O_3 addition in the regenerated samples, because the phase of MgO was exclusive and stable in the regenerated samples as shown in Figure 3.

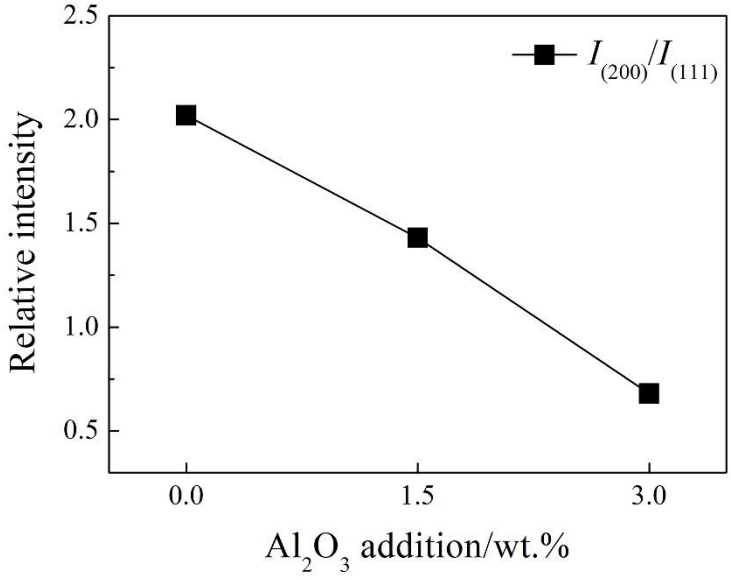

Figure 4. Relative intensities of $I_{CaO(200)}/I_{MgO(111)}$ of the sample A0, A1.5 and A3.0.

Figure 3 shows that the elements Fe and Al in the regenerated samples existed only in the C_4AF and C_3A phases. The standard reaction Gibbs energy of reactions between Fe_2O_3, Al_2O_3 and f–CaO which generate C_4AF and C_3A is shown in Figure 5 [19]. It shows that the phase of C_4AF generates preferentially when the impurity elements of Fe and Al exist concurrently, the phase of C_3A generates when there is excess Al element impurity (the mole ratio of Fe_2O_3 to Al_2O_3 < 1). Besides, preliminary study had proved that the phase of C_2F generates when the mole ratio of Fe_2O_3 to Al_2O_3 >1 [20].

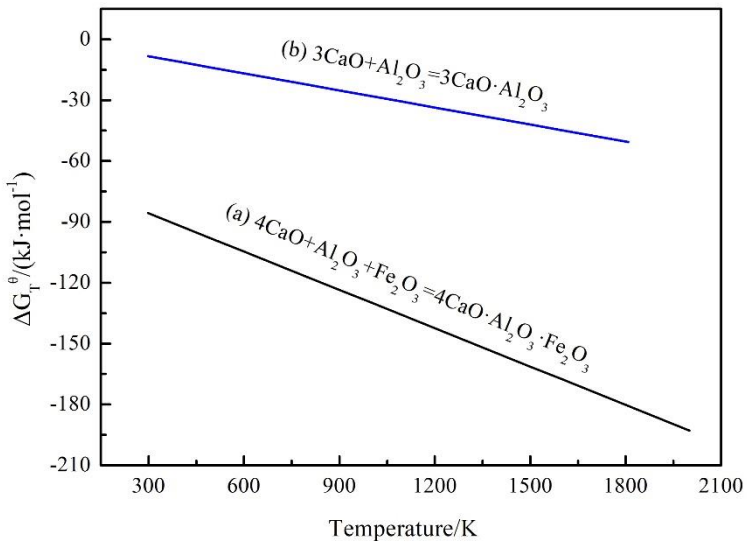

Figure 5. Standard reaction Gibbs energy of the reactions between Fe_2O_3, Al_2O_3 and f–CaO *vs.* temperature in the regenerated samples.

The theoretical content of the C_3S, C_4AF C_2F, C_3A and f–CaO phases (calcium–based phases) in the regenerated samples can be calculated by the Eq. (1) - (7) [21]. The results (as shown in Table 3) indicates that the theoretical content of the C_3A phase increased while that of the f–CaO phase

Preprints (www.preprints.org) | NOT PEER-REVIEWED | Posted: 14 September 2023 doi:10.20944/preprints202309.0890.v1

decreased as the increasing of Al_2O_3 addition, and the Fe element of the sample A1.5 and A3.0 all generated the C_4AF phase. These calculation results were identical with the phase compositions analysis shown in Figure 3.

$$w(C_3S) = 3.80w(SiO_2) \quad (1)$$

$$w(C_4AF) = 4.77w(Al_2O_3) \text{ (mole ratio of } Fe_2O_3 \text{ to } Al_2O_3 > 1) \quad (2)$$

$$w(C_4AF) = 3.04w(Fe_2O_3) \text{ (mole ratio of } Fe_2O_3 \text{ to } Al_2O_3 < 1) \quad (3)$$

$$w(C_2F) = 1.70[w(Fe_2O_3)-1.57w(Al_2O_3)] \quad (4)$$

$$w(C_3A) = 2.65[w(Al_2O_3)-0.64w(Fe_2O_3)] \quad (5)$$

$$w(\text{f–CaO}) = w(CaO)-1.10w(Al_2O_3)-0.70w(Fe_2O_3)-2.80w(SiO_2) \text{ (mole ratio of } Fe_2O_3 \text{ to } Al_2O_3 > 1) \quad (6)$$

$$w(\text{f–CaO}) = w(CaO)-1.65w(Al_2O_3)-0.35w(Fe_2O_3)-2.80w(SiO_2) \text{ (mole ratio of } Fe_2O_3 \text{ to } Al_2O_3 < 1) \quad (7)$$

$w(C_3S)$, $w(C_4AF)$, $w(C_2F)$, $w(C_3A)$, w(f–CaO)—the mass fraction of the calcium–based phases in the regenerated samples, wt.%;

$w(SiO_2)$, $w(Al_2O_3)$, $w(Fe_2O_3)$, $w(CaO)$—the mass fraction of the regenerated samples' composition, wt.%.

Table 3. Theoretical contents of each calcium–based phases in sample A0, A1.5 and A3.0 (wt.%).

Calcium–based phases	A0	A1.5	A3.0
C_3S	10.11	9.98	9.85
C_4AF	5.25	6.62	6.53
C_2F	0.82	0.00	0.00
C_3A	0.00	3.05	6.81
f–CaO	13.11	10.66	8.12

3.2. Microstructures of Regenerated Magnesia-Calcium Bricks

Figure 6(a) shows the SEM images of the regenerated samples' surfaces. The white phases shown in the selected areas *1*, *2* and *3* in Figure 6(a) were f–CaO, C_4AF or C_4AF–C_3A, and C_3S phases respectively, while the dark phases shown in Figure 6(a) were all MgO phase. Besides, it indicates that the phase of C_4AF and C_3A showed a tendency of aggregation in the sample A1.5 and A3.0. It is because that the elements of Fe and Al exist in the form of liquid phase at the firing temperature (1873 K), the C_3A phase (melting point of 1808 K [19]) and the C_4AF phase (melting point of 1688 K [22]) successively crystallized from the liquid phases, and sintered together during the furnace cooling process.

Figure 6(b) shows the SEM images of the regenerated samples' fractures. It shows that the sample A1.5 and A3.0 both present much more compactness than the sample A0, and the calcium–based phases were more continuous along with the increase of Al_2O_3 addition. Table 3 shows that the increase of C_3A content was the main change among that of the calcium–based phases as Al_2O_3 addition increasing. Therefore, it can prove that the generation of C_3A improved the sinterability of the regenerated samples.

Preprints (www.preprints.org) | NOT PEER-REVIEWED | Posted: 14 September 2023 doi:10.20944/preprints202309.0890.v1

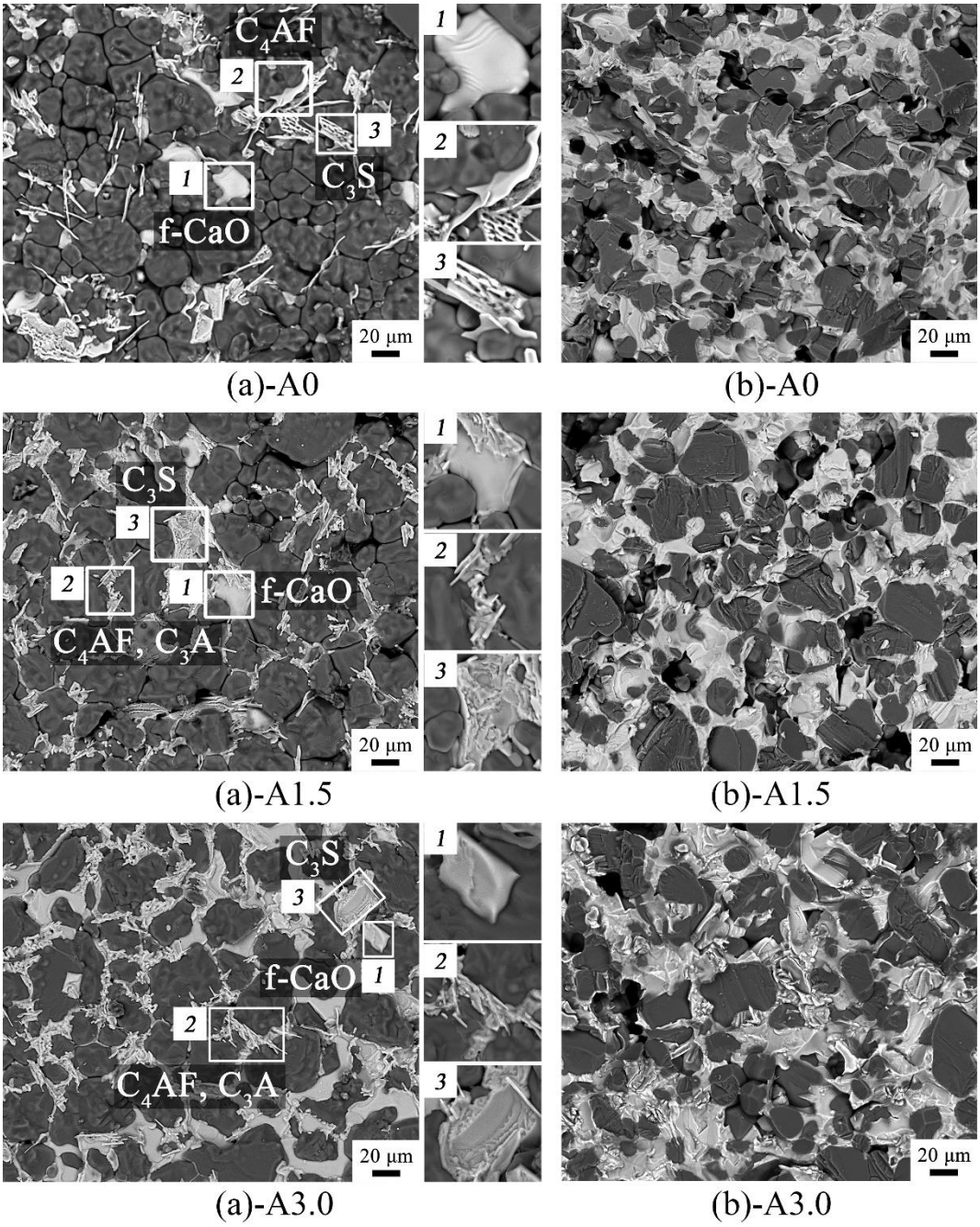

Figure 6. (**a**) SEM images of the regenerated samples' surfaces; (**b**) SEM images of the regenerated samples' fractures.

Figure 3 shows that there were too few of the C_3A phase to be observed in its character diffraction peak in the sample A1.5. It did not match the theoretical calculation as shown in Table 3. It is because that part of the Al element was dissolved into the C_3S phase, reducing generation of the C_3A phase [20]. The EDS analysis of the C_3S phase in Figure 6(a)–A1.5 is shown in Figure 7. It can be seen a significant solid solution appearing between the Al element and the C_3S phase.

Preprints (www.preprints.org) | NOT PEER-REVIEWED | Posted: 14 September 2023 doi:10.20944/preprints202309.0890.v1

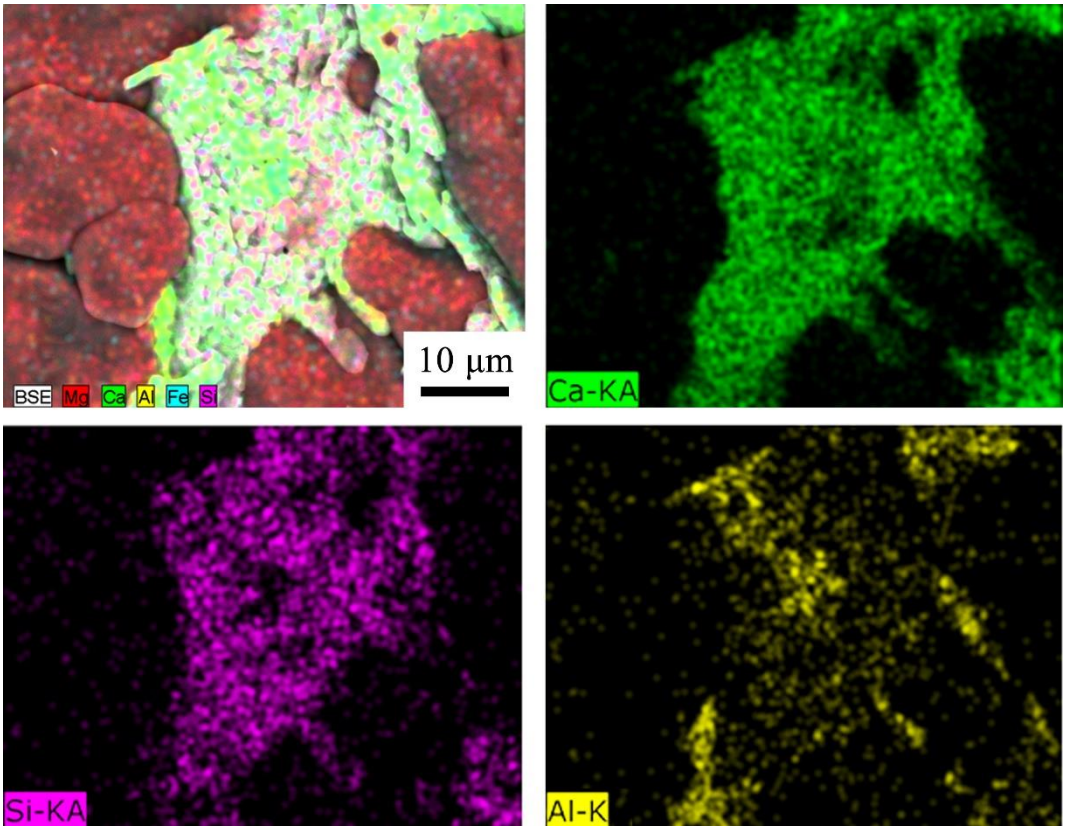

Figure 7. The elements of Ca, Si, Al distribution of the C_3S phase in the sample A1.5.

3.3. Room Temperature and Hot Flexural Strength of the Regenerated Magnesia-Calcium Bricks

Figure 8 shows the results of the room temperature and hot (1573 K) flexural strength of the samples A0, A1.5 and A3.0. It indicates that the room temperature flexural strength of the regenerated samples enhanced, oppositely, the hot flexural strength of the regenerated samples reduced with Al_2O_3 addition increasing. It is due to the increasing of the low melting point phases content (C_4AF and C_3A) as shown in Table 3 that improved the sinterability of the regenerated samples as shown in Figure 6, and subsequently enhanced their bulk density as shown in Figure 8. Thus, it results in the opposite phenomenon between the room temperature strength and the hot flexural strength of the regenerated samples with Al_2O_3 addition increasing.

Preprints (www.preprints.org) | NOT PEER-REVIEWED | Posted: 14 September 2023 doi:10.20944/preprints202309.0890.v1

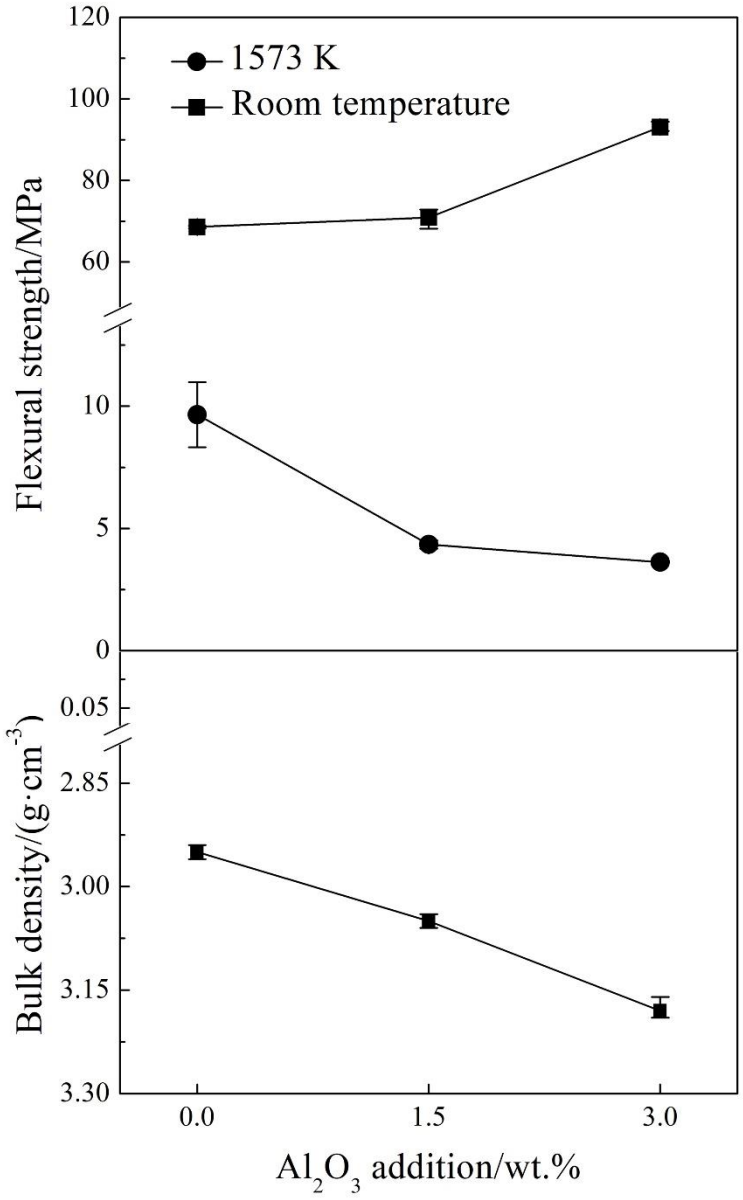

Figure 8. The room temperature and hot flexural strength, and the bulk density of the sample A0, A1.5 and A3.0.

3.4. Resistance to Cement Clinker Corrosion of the Regenerated Magnesia-Calcium Bricks

The SEM images of the sample A0, A1.5 and A3.0 cross-section after corrosion resistance experiment are shown in Figure 9(a)–(c). It indicates that the cement clinker corrosion to the regenerated samples was gradually serious as the increasing of Al_2O_3 addition, and the cement clinker was more prone to corroding the regenerated samples along their calcium–based phases. It is because that the calcium–based phases of the regenerated samples were composed of the C_3S, C_4AF, C_3A and f–CaO phases, among which the phases of C_4AF and C_3A content increased with Al_2O_3 addition increasing. It improved the wettability of the regenerated samples, and thus, the melting cement clinker was much easier to corrode the regenerated samples along the areas of these low melt point phases [red arrow pointing out in Figure(a)–(c)] as they all exist in liquid phase form at 1823 K. Figure 9(d) shows an increasing tendency of the regenerated samples' coating adherence along with the increase of Al_2O_3 addition. It is because that the reaction areas between the cement clinker and regenerated samples increase with additive Al_2O_3 increased, resulting in their strength of coating adherence enhanced.

Preprints (www.preprints.org) | NOT PEER-REVIEWED | Posted: 14 September 2023 doi:10.20944/preprints202309.0890.v1

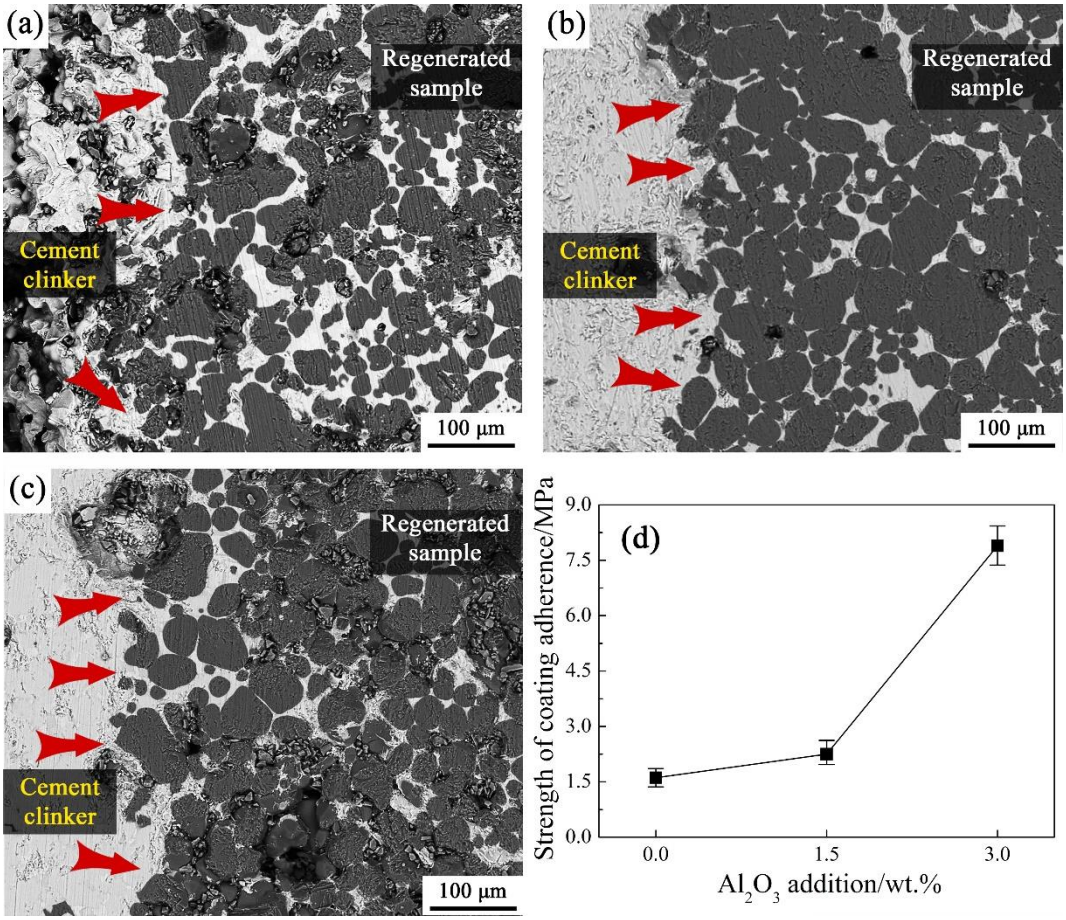

Figure 9. SEM images of the regenerated samples' cross-section after corrosion resistance experiment: (**a**) sample A0; (**b**) sample A1.5; (**c**) sample A3.0; (**d**) strength of coating adherence of the sample A0, A1.5 and A3.0.

The corrosion of the cement clinker to the phase of MgO was carried out by an elements distribution scanning analysis across their contact areas as shown in Figure 10(a). The analysis results indicate that a reaction layer containing element Ca, Si and Mg existed in the interfacial surface of these contact areas. The thickness *d* of the reaction layer gradually became larger with Al_2O_3 addition increasing as shown in Figure 10(b), which also indicates an aggravating corrosion of the cement clinker to the phase of MgO.

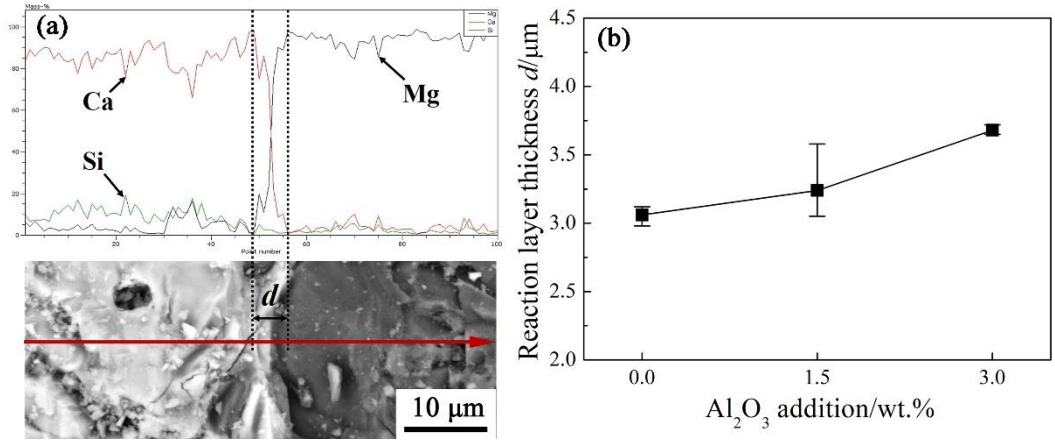

Figure 10. (**a**) The elements distribution scanning analysis across the contact area of the cement clinker and the MgO phase; (**b**) reaction layer thickness *d* of the sample A0, A1.5 and A3.0.

 doi:10.20944/preprints202309.0890.v1

Generally, Al_2O_3 addition had a positive effect on the room temperature performances of the regenerated samples, such as the bulk density and the room temperature flexural strength, on the contrary, it had an adverse effect on the high-temperature performances of the regenerated samples, such as the hot flexural strength and corrosion resistance except of the strength of coating adherence, because of the low melting point phases of C_4AF and C_3A generating. It had been reported that the room temperature flexural strength and the strength of coating adherence of the chromium–free refractories applied on cement rotary kiln were lager than 21.60 MPa and 0.52 MPa [23], in comparison that of sample A0, A1.5, A3.0 were 68.58 MPa, 70.91 MPa, 93.11 MPa and 1.61 MPa, 2.25 MPa, 7.89 MPa accordingly. It shows that sample A0, A1.5, A3.0 could all meet the room temperature flexural strength and the strength of coating adherence. However, the hot flexural strength of sample A0, A1.5, A3.0 was 9.65 MPa, 4.34 MPa, 3.62 MPa respectively, and it shows that the hot flexural strength of sample A0 was only higher than that of the literature report (lager than 5.4 MPa) [24]. Therefore, the sample A0 can be considered as most suitable regenerated sample for cement rotary kiln, and the content of Al_2O_3 in the regenerated magnesia-calcium brick should not be higher than 1.1 wt.% (without extra Al_2O_3 addition).

4. Conclusions

The magnesia-calcium brick samples were prepared by using spent magnesia-calcium brick, fused magnesia and Al_2O_3 powder additive as the main raw materials, liquid paraffin as the binder, and firing at 1873 K for 2 h under an air atmosphere respectively, among which the Al_2O_3 powder addition was 0 wt.%, 1.5 wt.%, 3.0 wt.%. The main phase compositions of the sample A0 and A1.5 were MgO, f–CaO, C_3S, C_4AF, and a new phase C_3A was observed in the sample A3.0 besides MgO, f–CaO, C_3S, C_4AF. There was a solid solution appearance between the Al element and the C_3S phase, resulting in the actual content of the C_3A phase was lower than the theoretical calculation, and it led to the phase of C_3A being not observed in the sample A1.5. The room temperature performances of the regenerated samples such as bulk density and flexural strength enhance along with the increase of Al_2O_3 addition, since the low melting point phases of C_4AF and C_3A content increase which improve the sinterability of the regenerated samples. However, the high-temperature performances of the regenerated samples such as hot flexural strength (1573 K) and corrosion resistance (1823 K) degrade as the addition of Al_2O_3 increasing, because the melting points of the C_4AF and C_3A phases were close to 1573 K, furthermore, they were in liquid phase form at 1823 K that wetted the regenerates sample to enhance the reaction between the cement clinker and the MgO phase, resulting in the increasing of the strength of coating adherence. The sample A0 can be considered as most suitable regenerated sample for cement rotary kiln, as comparing the main performances with other chromium–free refractories for cement rotary kiln, that is, the total content of Al_2O_3 in the regenerated magnesia-calcium brick should be no more than 1.1 wt.%.

Author Contributions: Conceptualization, Q.G.-B. and Z.M.; methodology, Q.G.-B., H.Y.-D. and Z.M.; software, Q.G.-B. and W.H.-G.; validation, H.J. and Z.X.-H.; formal analysis, Q.G.-B. and H.J.; investigation, Q.G.-B., H.Y.-D. and P.B.; resources, H.J. and P.B.; data curation, Q.G.-B., W.H.-G. and Z.X.-H.; writing—original draft preparation, Q.G.-B.; writing—review and editing, Z.M., H.Y.-D. and W.H.-G.; visualization, Q.G.-B., H.J. and Z.X.-H.; supervision, P.B. and Z.M.; project administration, Q.G.-B. and P.B. All authors have read and agreed to the published version of the manuscript.

Institutional Review Board Statement: Not applicable.

Informed Consent Statement: Not applicable.

Data Availability Statement: Not applicable.

Acknowledgments: This work was supported by 2023 Zhanjiang Ocean Young Talent Innovation Project of China (2023E0009) and National Natural Science Foundation Outstanding Youth Science Fund project of China (52322806).

Conflicts of Interest: The authors declare no conflict of interest.

References

1. Nievoll, J.; Guo, Z.Q.; Shi S. Performance of magnesia hercynite bricks in large Chinese cement rotary kilns, *RHI Bulletin*, **2006**, 3, 15–17.
2. Schacht, C. Refractories Handbook; CRC Press: Boca Raton, FL, USA, 2004, p. 607.
3. Driscoll, M.O. Price temper steel market promise. *Ind. Miner.* **1994**, 324, 35–49.
4. Guo, M.; Jones, P.T.; Parada, S.; Boydens, E.; Dyck, J.V.; Blanpain, B.; Wollants, P. Degradation mechanisms of magnesia–chromite refractories by high–alumina stainless steel slags under vacuum conditions. *J. Eur. Ceram. Soc*. **2006**, 26, 3831–3843.
5. Gómez–Rodríguez, C.; Antonio–Zárate, Y.; Revuelta–Acosta, J.; Verdeja, L.F.; Fernández–González, D.; López–Perales, J.F.; Rodríguez–Castellanos, E.A.; García–Quiñonez, L.V.; Castillo–Rodríguez, G.A. Research and development of novel refractory of MgO doped with ZrO_2 nanoparticles for copper slag resistance. *Materials*. **2021**, 14, 2277.
6. Zhu, B.Q.; Fang, B.X.; Zhang, W.J.; Li, X.C.; Wan, H.B. Corrosion mechanism of ladle furnace refining slag to fired MgO–CaO bricks. *China's refractories*, **2010**, 019, 1–4.
7. Wei, Y.W.; Li, N. Refractories for clean steel making. *Am. Ceram. Soc. Bull.* **2002**, 81, 32–35.
8. Qiu, G.B.; Peng, B.; Guo, M.; Zhang, M. Regeneration utilization of spent MgO–CaO bricks for argon oxygen decarburization furnace. *J. Chin. Ceram. Soc.* **2013**, 41, 1284–1289.
9. Soltanieh, M.; Payandeh, Y. Relationship between oxygen chemical potential and steel cleanliness. *J. Iron Steel Res. Int.* **2005**, 12, 28–33, 62.
10. Rabah, M.; Ewais, E.M.M. Multi–impregnating pitch–bonded Egyptian dolomite refractory brick for application in ladle furnaces. *Ceram. Int.* **2009**, 35, 813–819.
11. Chen, S.J.; Tian, L.; Li, G.H.; Tian, F.R. MgO–CaO refractories, Ed. by L. Song, Metallurgical Industry Press, Beijing, China, 2012; pp. 25, 52–57.
12. Yu, J.K.; Dai, W.B. Influence of fine α–Al_2O_3 powder on the properties of the magnesia–calcia refractories. *J. Northeast. Univ. (Natural Science)*, **2003**, 24, 1068-1070.
13. Shahraki, A.; Ghasemi–Kahrizsangi, S.; Nemati, A. Performance improvement of MgO–CaO refractories by the addition of nano–sized Al_2O_3. *Mater. Chem. Phys.* **2017**, 198: 354–359.
14. Qiu, G.B.; Peng, B.; Li, X.; Guo, M.; Zhang, M. Hydration resistance and mechanism of regenerated MgO–CaO bricks. *J. Ceram. Soc. Jpn*. **2015**, 123, 1–6.
15. Liang, Y.B.; Shen, X.L. Effects of spent MgO–CaO bricks additive amount on the properties of baking MgO–CaO bricks, *Refractories*, **2008**, 42, 392–393.
16. Zhang, W.; Shi, G.; Wei, F.C.; Wang, C.Y. Preparation of magnesia–calcia dry mix from used MgO–CaO bricks, *Refractories*, **2012**, 46, 126–128.
17. Yang, W.Z.; Chen, S.J.; Wei, Z.L.; Zhang, F.Q. Effect of Al_2O_3 additions on characteristic of burned magnesia–calcia brick. *J. Anshan Univ. Sci. Technol.* **2003**, 26, 425–428.
18. Cheng, X.; Liu, L.; Xiao, L.H.; Huo, X.T.; Guo, M.; Zhang, M., Effect of MgO on corrosion mechanism under LF refining slag for MgAlON–MgO composites synthesized from spent MgO–C brick: Wetting behaviour, reaction process and infiltration mechanism. *J. ALLOY. COMPD.* **2023**, 963, 171278.
19. Zhu, Z.P.; Jiang, T.; Li, G.H.; Guo, Y.F.; Yang Y.B. Thermodynamics of reactions among Al_2O_3, CaO, SiO_2 and Fe_2O_3 during roasting processe. Thermodynamics–Interaction Studies–Solids, Liquids and Gases, Chapter 30; Moreno–pirajan, InTech, 2011, 825–838.
20. Qiu, G.B.; Peng, B.; Yue, C.S.; Guo, M.; Zhang, M. Properties of regenerated MgO–CaO refractory bricks: impurity of iron oxide. *Ceram. Int.* **2016**, 42, 2933–2940.
21. Sun, Y.F.; Wang, X.M.; Wang, C. X.; Sun, P.Q. Magnesia and magnesium matrix composite refractories; Metallurgical Industry Press, Beijing, 2010, pp. 25, 32.
22. Taschler, T. Refractory materials for the copper and lead industry, In *Tehran International Conference on Refractories*; Iran, 2004; pp. 302–320.
23. Wang, Z.F.; Chen, J.; Wang, X.T.; Zhang, B.G.; Liu, H. Effects of rare earth oxides on physical properties and coating adhering performance of magnesia refractories. *J. Wuhan Univ. Sci. Technol.* **2010**, 33, 595–598.
24. Zhang, B.X. Research on non–chromium refractory for rotary cement kiln in burning zone. Master Dissertation, University of Science and Technology Liaoning, Anshan Liaoning, 2008.